광산지질 16권 4호(1983) pp. 269—276

Three-Dimensional Standard Curves in Induced Polarization Method

Hee Joon Kim*

Abstract: This paper describes three-dimensional (3-D) standard curves for single prismatic buried bodies in induced polarization (IP) method. Dipole-dipole IP responses for the bodies are calculated by the numerical modeling technique using an integral equation solution.

The pattern of IP responses for conductive targets depends on the ratio of the width of body to the depth extent. The IP response of a body of six units in strike length approximates that of a two-dimensional body. In addition, if the strike length is long enough, a layered-earth interpretation is applicable for a body much longer than four units in width. Moving an IP line away from the center of a body alon gstrike produces an effect similar to that of increasing the depth. Moving the location of body along line has little effect to the pattern of IP responses.

Introduction

The solution of 3-D IP problems is essential in designing effective IP surveys and interpreting IP data in many field environments. In the past decade, substantial advances have been made in this direction through numerical modeling techniques for 3-D geologic structures. Althoughthe 3-D numerical modelings associated with finite-difference (Endo et al., 1974; Dey and Morrison, 1979) and finite-element (Pridmore et al., 1981) methods are preferable for modeling complex geologies, they requires large computer time and strage. In practice, therefore, integral equation methods (Dieter et al., 1969; Hohmann, 1975; Endo et al., 1979) are useful and one of the most cost-effective ones for simple 3-D models.

The purpose of this paper is to show the effects of changes in a number of model parameters on the IP responses of prismatic bodies. These 3-D IP standard curves are calculated by the integral equation method (Endo et al., 1979). Understanding the effects of parameter changes for simple models is a prerequisite in interpreting the responses over complex geologies. Numerical results would, of course, include both IP and apparent resistivity responses. However, on account of limited space, only IP responses are shown for all of the models.

*Department of Applied Geology, National Fisheries University of Busan Busan 608, Korea

Fundamental equation and IP effect

A typical integral equation for inhomogeneities with uniform resistivities was developed by Snyder (1976). In the case of a simple body characterized by uniform resistivity ρ_2 in an otherwise uniform half-space of resistivity ρ_1, using an appropriate Green's function G, a potential ϕ is given by

$$\phi(\boldsymbol{r}, \boldsymbol{r}_s) = \frac{\rho_1 I}{4\pi} G(\boldsymbol{r}, \boldsymbol{r}_s) + \frac{1}{4\pi} \iint_s q(\boldsymbol{r}') \cdot G(\boldsymbol{r}, \boldsymbol{r}') ds', \quad \cdots\cdots(1)$$

where

$$q = 2\frac{\rho_2 - \rho_1}{\rho_2 + \rho_1} \boldsymbol{n} \cdot \nabla\phi, \quad \cdots\cdots(2)$$

$\boldsymbol{r}$ is denotes the field point, $\boldsymbol{r}_s$ the position of pole source, $\boldsymbol{r}'$ the position of surface elements ds', I the strength of current source located at the point $\boldsymbol{r}_s$, q the surface charge density of inhomogeneity, and $\mathbf{n}$ the outward unit vector normal to the boundary surface S. The Green's function for the half-space is

$$G(\boldsymbol{r}, \boldsymbol{r}') = \frac{1}{|\boldsymbol{r}-\boldsymbol{r}'|} + \frac{1}{|\boldsymbol{r}-\boldsymbol{r}''|}, \quad \cdots(3)$$

where $\boldsymbol{r}''$ is the reflected point of $\boldsymbol{r}'$ across the half-space boundary. Applying the method of moments (Harrington, 1968), equation (1) is solved numerically (e.g., Endo et al., 1979).

An IP effect is calculated by allowing the resistivities of the model to be complex numbers. The intrinsic IP response (θ_i) of the body is taken as the phase of the complex resistivity (Van Voorhis et al., 1973). The phase of complex potential difference measured between receiving electrodes is taken as the apparent IP response (θ_a). In this paper, the IP response is interpreted as the percentage of the intrinsic IP response of the body:

$$B_2(\%) = \theta_a/\theta_i \times 100. \quad \cdots\cdots(4)$$

This interpretation is consistent with the "*B*" factor introduced by Seigel (1959).

Numerical results

Fig. 1 shows a prismatic model. The earth except for a rectangular body having resistivity ρ_2 is taken to be a half-space of resistivity ρ_1. The basic model parameters are width (W), strike length (SL), depth extent (DE) and depth (D). Other parameters considered here are body position along line (PX) and line position along strike (PY). Only the dipole-dipole array is considered in this paper, because the dipole-dipole array usually gives the largest anomalies and has the best overall resolution (Coggon, 1973). As usuall, all dimensions are in units of *a*, dipole length. IP responses up to five units of dipole separation are shown in pseudo-sections for all of the models. The ratio of polarizable body resistivity (ρ_2) to earth resistivity (ρ_1) is fixed to $\rho_2/\rho_1 = 3.0/12.5$.

1. Width

Fig. 2 (W=1, 2, 3 and 4) shows how the width affects the response associated with a body that is 2 units in strike length and 2 in depth extent. The depth to the top of body is 1 unit and the IP

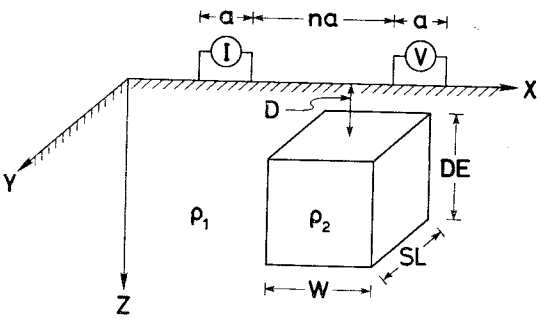

Fig. 1 Three-dimensional model. The earth except for a polarizable rectangular body of resistivity ρ_2 is taken to be a half-space of resistivity ρ_1. All dimensions are in units of a, dipole length. W: width, SL: strike length, DE: dedth extent, D: depth, I: current dipole and V: potential dipole.

line is taken at the center of body bisecting the strike in the plan view.

The pattern of IP responses varies when the width increases to two units, with the anomaly becoming broader and larger in amplitude. In the case of thin body (W < DE), the appearing position of the highest anomaly coincides with the location of body in the pseudo-section. In the cace of thick bodies (W ≥ DE), however, the highest anomalies appear at the both outsides of bodies, so sophisticated interpretation techniques are required in actual field data.

In the case of W = 4, nearly the same values appear in the inside of body for each dipole separation less than three units in the pseudo-section. This is almost the same tendency as the response of three-layer-earth, but the amplitude is small because the strike length of body is short. The effect of strike length will be discussed in the following section. If the strike length is long enough, therefore, one-dimensional (layered-earth) interpretations can be applicable for the body much longer than four units in width. Note that, even in this case, the influence of the side wall of body appears at the bottom of the body in the pseudo-section, and the values at those points diverge.

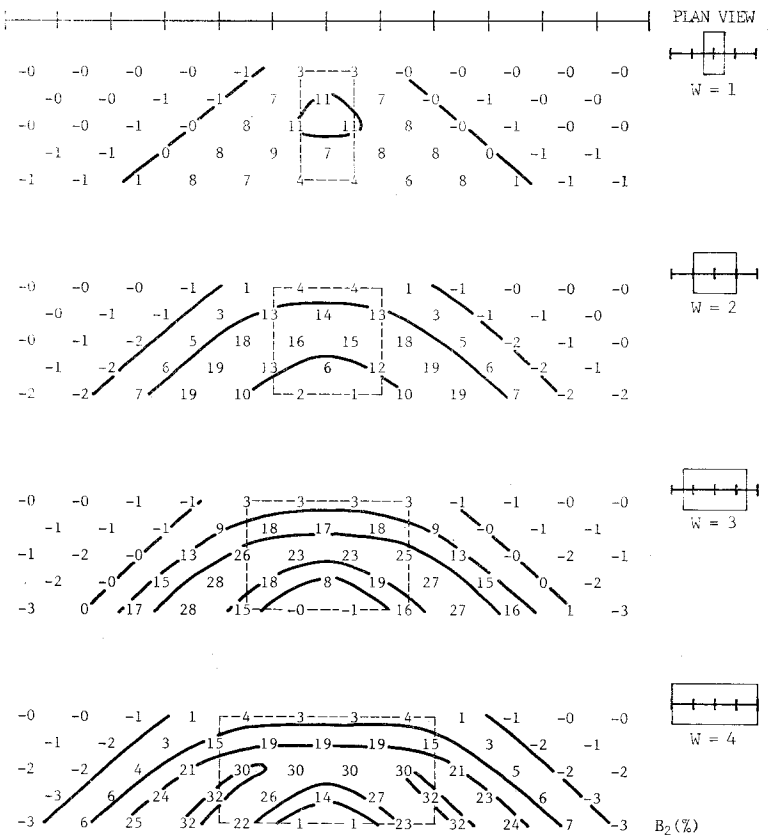

Fig. 2 Effect of width (W=1, 2, 3 and 4) on IP responses; SL=2, DE=2, D =1 and ρ_2/ρ_1=3.0/12.5.

2. Strike length

Fig. 3 shows IP responses for the strike length of 2, 4, 6 and 8 units. In each case the width of body is 2 units, the depth extent 2, the depth 1 and the IP line bisects the strike of body in the plan view.

The patterns of IP responses are almost the same in spite of the changes of strike length. There is a large increase in IP response as the strike length increases from two to four by six units, but only a small change when the strike length increases further. This shows that the IP response of a six or so units long can be approximated by a two-dimensional body for all pratical applications. Such approximation, however, is limited when the IP line does not bisect the strike of body, or when the body is very conductive (Hohmann, 1975).

3. Depth extent

Fig. 4 shows IP responses for the depth extents of 1, 2, 3 and 4 units. In each case the width of body is 2 units, the strike length 2, the depth 1 and the IP line bisects the strike of body in the plan view.

The most important effect of the depth extent appears at the points of the bottom center in the pseudo-section. In other words, the change of depth extent is recognized when current and potential dipoles straddle the body at the large dipole separations. The depth extent of body seems to be detectable by the negative anomalies appearing at the points of the bottom center in

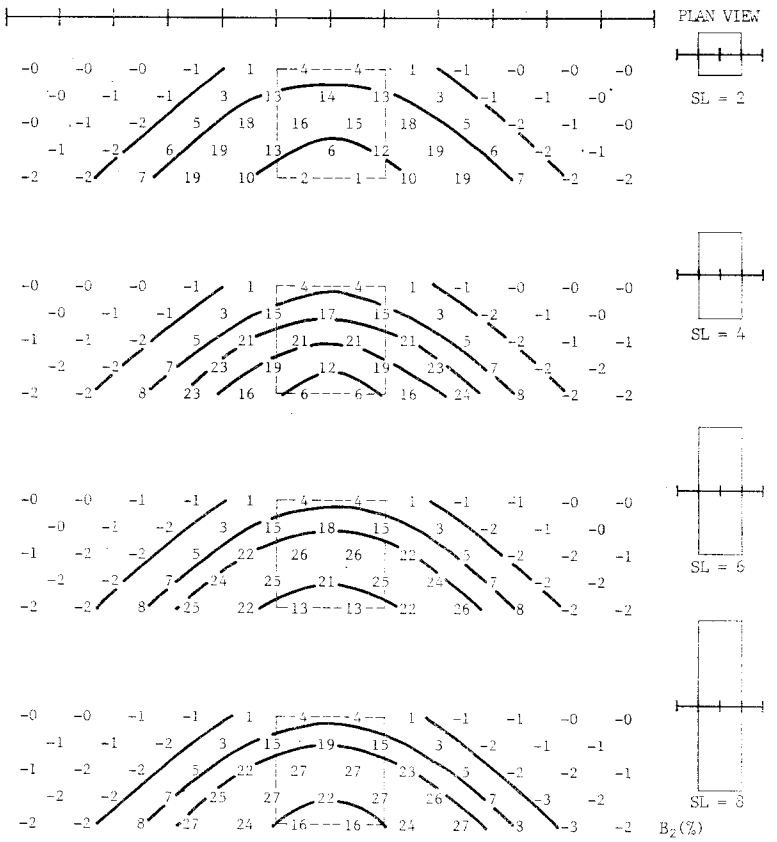

Fig. 3 Effect of strike length (SL=2, 4, 6 and 8) on IP responses; W=2, DE =2, D=1 and ρ_2/ρ_1=3.0/12.5.

the pseudo-section.

The pattern of IP responses varies when the depth extent increases to three or four units. From Figs. 2 and 4, it is found that the pattern of IP responses is mainly determined by the ratio of the width to the depth extent for this resistivity ratio, except the case that the depth extent is slightly larger than the width (DE = 3).

4. Depth

Fig. 5 shows IP responses for the depths of 0.5, 1, 1.5 and 2 units. The size of body is 2×2×2 units and the IP line bisects the strike of body in the plan view.

IP responses significantly decrease as the depth increases. In general, deeper bodies give rise to broder, lower-amplitude anomalies. It is because that the current density at the surface of body generated by a source dipole becomes small as the depth increases.

One of the most important source parameters to be determined in exploration is the depth of targets. From Fig. 5, it is found that dipole-dipole data are very diagnostic for the information of depth.

5. Body position along line

Fig. 6 compares the IP responses of a centered body (PX = 0) with those for two other body positions (PX = 0.25 and 0.5). The size of body is 2 × 2 ×2 units, the depth is 1 and the IP line bisects the strike of body in the plan view.

While the magnitudes of IP responses are slightly different, the patterns are about the same. This

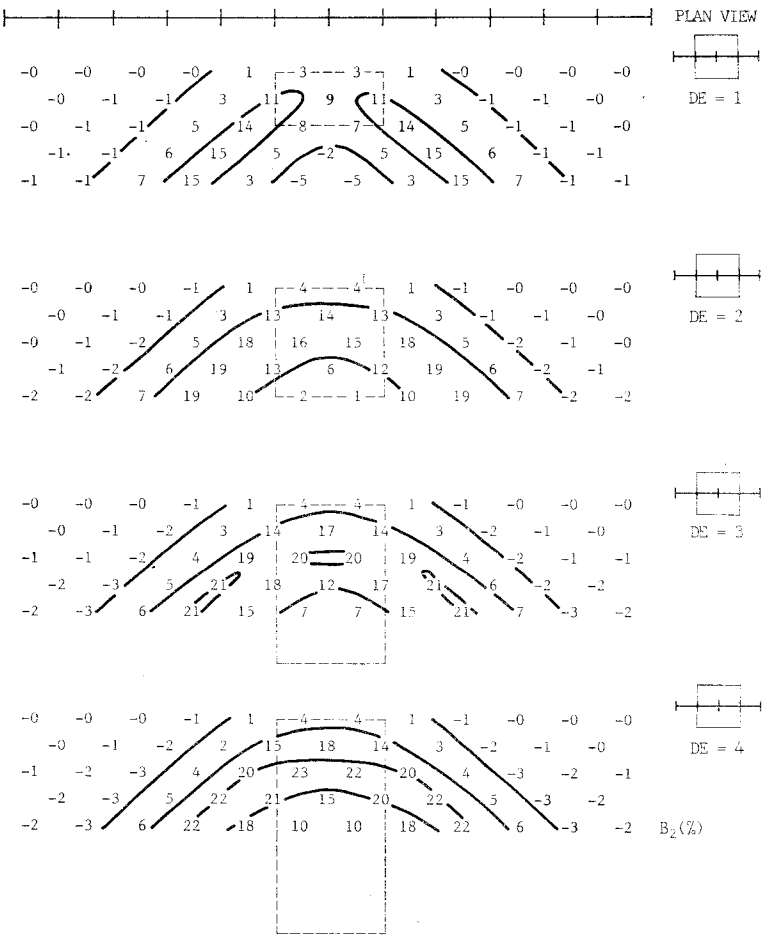

Fig. 4. Effect of depth extent (DE=1, 2, 3 and 4) on IP responses; W=2, SL=2, D=1 and ρ_2/ρ_1=3.0/12.5.

shows that the position of body along line has little effect to the pattern of IP responses.

6. Line position along strike

Fig. 7 shows the effect of moving the IP line along strike. The size of body is 2×2×2 units and the depth is 1. Results are shown for four positions: at the center of the body, at the end of the body, and at one and two units off the end of the body.

The effect of moving the line away from the center is similar to that of increasing the depth of body. The reason of that is also the same as the case of the depth change. This shows that, with only one pseudo-section, it would be impossible to deduce whether the body were buried directly beneath the line or off to one side.

Discussion and Conclusions

In the interpretation of field data, interpreters usually pay attention to the position of the highest anomaly or to the pattern of IP responses. From Figs. 2 and 4, for the conductive targets such as considered here, it is found that the pattern of IP responses depends on the ratio of the width of body to the depth extent. In the case of thin bodies, the appearing position of the highest anomaly coincides with the location of body in pseudo-section, so it is relatively easy to predict

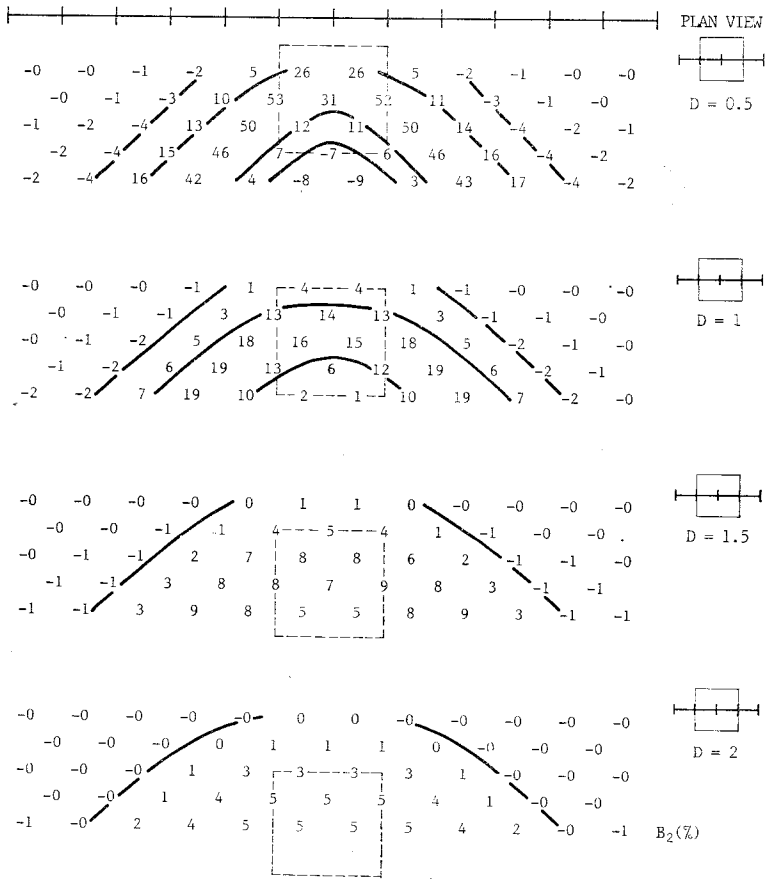

Fig. 5 Effect fo depth (D=0.5, 1, 1.5 and 2) on IP responses; W=2, SL=2, DE=2 and ρ_2/ρ_1=3.0/12.5.

the location of target in actual field data. In the case of thick bodies, however, the highest anomaly does not appear at the location of body, so sophisticated interpretations are needed. Note that the pattern of IP responses also varies with the array used (Yoshizumi, 1966) or with the resistivity ratio between target and its surrounding medium (Yamamoto et al., 1980).

From Figs. 5 and 7, it is found that moving the IP line away from the center of the body produces an effect similar to that of increasing the depth of body. This means that, with only one field data of pseudo-section, it is impossible to determine the location of target. Such difficulty may be solved by the method of 3-D analysis using IP curves of both plane and profile (Takeuchi et al., 1974).

Numerical solution of the integral equation involves full matrices that are smaller than the large bounded, sparses matrices encountered with finite-difference or finite-element techniques. These techniques which divide the entire half-space into a mesh are probably preferable for modeling complex geologic structures. The integral equations, on the other hand, are most useful for modeling a series of simple bodies, because the matrices are small and it is not necessary to change the mesh between models. Pridmore et al. (1981),for example, shows that the integral equation method is about twenty times faster than the finite-element method for a cubic model.

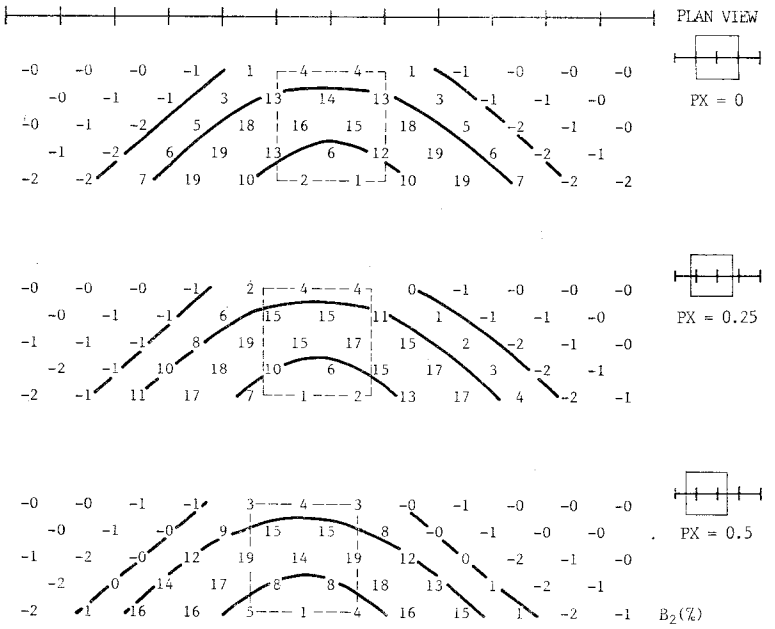

Fig. 6 Effect of body position (PX=0, 0.25 and 0.5) along line on IP responses; W=2, SL 2, DE=2, D=1 and ρ_2/ρ_1=3.0/12.5.

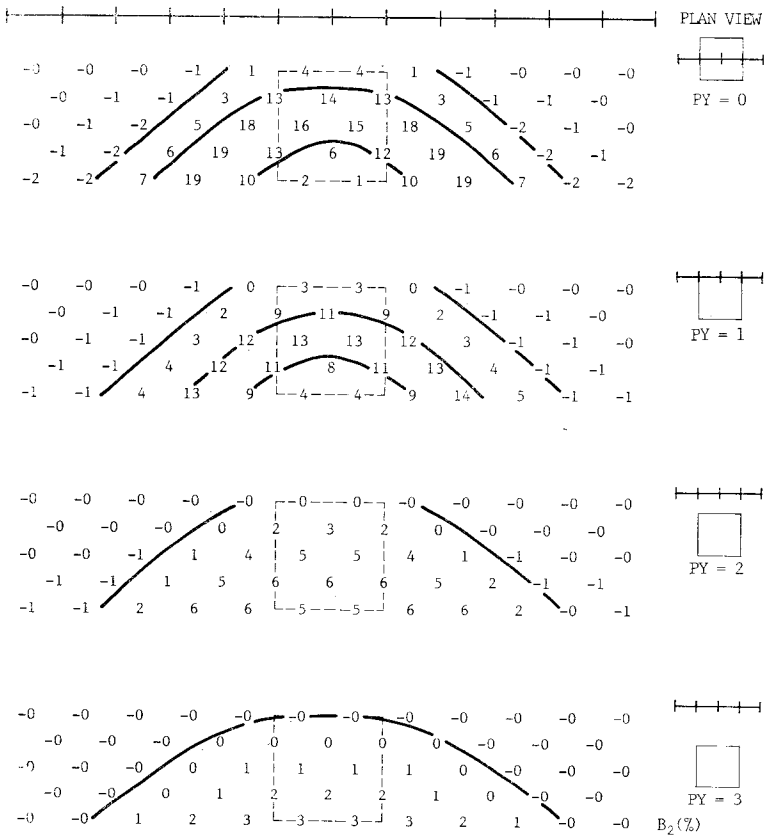

Fig. 7 Effect of line position (PY=0, 1, 2 and 3) along strike on IP responses the same body as in Fig. 6.

Acknowledgments

This research has been supported by the Korean Science & Engineering Foundation; this support is gratefully acknowledged.

References

Coggon, J. H., 1973: A comparison of IP electrode arrays, Geophysics, **38** (4), 737–761.

Dey, A. and H. F. Morrison, 1979: Resistivity modeling for arbitrarily shaped three-dimensional structures, Geophysics, **44** (4), 753–780.

Endo, G., M. Takeuchi and S. Matsuzaka, 1974: Study on the three-dimensional modeling of strata in electrical prospecting (In comparison with the result of the three-dimensional numerical calculation of modeling of strata), Butsuri-Tanko, **27** (3), 95–102. (in Japanese)

Endo, G., Y. Yamamoto, M. Takeuchi and K. Noguchi, 1979: On the numerical calculation method using an integral equation solution (I), Butsuri-Tanko, **32** (3), 117–125. (in Japanese)

Harrington, R. F., 1968: Field Computation by Moment Methods, New York, Macmillan Co., 229p.

Hohmann, G. W., 1975: Three-dimensional induced polarization and electromagnetic modeling, Geophysics, **40** (2), 309–324.

Pridmore, D. F., G. W. Hohmann, S. H. Ward and W. R. Sill, 1981: An investigation of finite-element modeling for electrical and electromagnetic data in three dimensions, Geophysics, **46** (7), 1009–1024.

Seigel, H. O., 1959: Mathematical formulation and type curves for induced polarization, Geophysics, **24** (3), 547–565.

Snyder, D. D., 1976: A method for modeling the resistivity and IP response of two-dimensional bodies, Geophysics, **41** (5), 997–1015.

Takeuchi, M., K. Noguchi and G. Endo, 1974: Study on the three-dimensional modeling of strata in electrical prospecting (In the case of induced polarization method), Butsuri-Tanko, **27** (5), 189–200. (in Japanese)

Van Voorhis, G. D., P. H. Nelson and T. L. Drake, 1973: Complex resistivity spectra of porphyry copper mineralization, Geophysics, **38** (1), 49–60.

Yamamoto, Y., M. Takeuchi, K. Noguchi and G. Endo, 1980: On the numerical calculation method using an integral equation solution (II) (Analyses of the standard curves in IP method), Butsuri-Tanko, **33** (2), 57–62. (in Japaneses)

Yoshizumi, E. and T. Irie, 1966: Standard curves in induced polarization method), Butsuri-Tanko, **19** (4, 5), 133–145. (in Japanese)

IP法의 3次元 標準曲線

金 喜 俊

요약 : 단순한 四角柱型 物體에 대한 3차원 표준곡선을 해석하였다. 이들 표준곡선은 雙極子配置에 대하여 積分方程式을 이용한 數値計算技術로 구하였다.

電導性 물체에 대한 IP 應答은 물체의 폭과 두께의 비율에 따라서 그 패턴이 달라진다. 走向길이가 雙極子間隔의 6배 이상이 되면 2차원의 결과와 유사하다. 또한 走向길이가 길고, 폭이 쌍극자 간격의 4배이상이 되면 層構造(1차원) 해석도 가능하게 된다. 한편, 測線이 走向方向을 따라서 물체의 중심으로부터 멀어지는 효과는 물체의 깊이가 지표로부터 깊어질 때와 비슷하게 나타난다. 물체가 測線下에서 측선과 平行한 방향으로 이동하더라도 IP 패턴에는 거의 영향을 미치지 않는다.